Surface Reactivity and Plasma Energetics of SiH Radicals during Plasma Deposition of Silicon-Based Materials

W. M. M. Kessels,[†] Patrick R. McCurdy,[‡] Keri L. Williams, G. R. Barker, Vincent A. Venturo,[§] and Ellen R. Fisher*

Department of Chemistry, Colorado State University, Fort Collins, Colorado 80523-1872

Received: October 19, 2001

The surface reactivity of the SiH radical was measured during plasma deposition of various silicon-based materials using the imaging of radicals interacting with surfaces (IRIS) method. In this technique, spatially resolved laser-induced fluorescence (LIF) is used to determine surface reaction probabilities, R or β, of plasma species. For SiH, R is near unity, 0.96 ± 0.04, and shows no dependence on the gas mixture (SiH_4, Si_2H_6, SiH_4/H_2, Si_2H_6/H_2, SiH_4/NH_3, SiH_4/N_2, and SiH_4/CH_4) or on the plasma conditions used. The velocity of SiH in the molecular beam has also been measured, yielding the SiH kinetic translational temperature in the plasma. Modeling of the kinetic data yields an average SiH translational temperature of ~1100−1200 K for both SiH_4 and Si_2H_6 plasmas, which is nearly independent of the applied rf plasma power. The rotational temperature determined from the SiH rotational spectrum is ~600 K for both plasmas, also with no clear dependence on applied power. The difference in these temperatures is explained by examining energy dissipation in the inductively coupled plasma, suggesting that the translational temperature of SiH is determined by the excess energy released during the dissociation of SiH_4 or Si_2H_6 by electron impact.

I. Introduction

Plasma-enhanced chemical vapor deposition (PECVD) using SiH_4 and Si_2H_6 glow discharges is widely applied technologically for the production of a variety of silicon-based materials.[1,2] Hydrogenated amorphous silicon (a-Si:H) deposited from pure SiH_4 and Si_2H_6 has its primary applications in a-Si:H solar cells, in thin film transistors (TFTs) for liquid crystal displays, and in detectors.[3] SiH_4/H_2 and Si_2H_6/H_2 mixtures are used for the deposition of microcrystalline silicon solar cells and low-temperature deposition of polysilicon as a gate material in TFTs.[3,4] Hydrogenated amorphous silicon nitride (a-SiN_x:H) films deposited from SiH_4/NH_3 and SiH_4/N_2 plasmas are found in microelectronics as diffusion barriers, gate dielectrics in TFTs, and as a storage material for memory devices.[5] Furthermore, it is also used as antireflection and passivation coatings for crystalline silicon solar cells. Hydrogenated amorphous silicon carbide (a-SiC_x:H), for example deposited from SiH_4/CH_4 mixtures, is used in high-voltage and high-temperature electronic devices, p-type window layers in a-Si:H solar cells, and blue light emitting diodes (LEDs).[6]

The material properties of these silicon-based films are usually dependent on the plasma parameters, implying that film properties are partially determined by the contribution of different plasma species to film growth. Therefore, numerous studies have been performed on plasma reactions and on gas-phase densities of the different species in silane-based plasmas. These studies have focused primarily on plasma radicals, because it has become widely accepted that neutral radical species are the dominant contributors to thin film deposition of silicon-based materials.[1] In general, less attention has been afforded to the surface interactions of plasma species, although their contribution to film growth is directly dependent on radical sticking probability or surface reactivity. Indeed, a high gas-phase density of a certain radical can be the result of favored production of this radical, but it can also be attributed to a very low surface reactivity and consequently low (surface) loss. This implies that limited conclusions can be drawn on the relevancy of plasma species to the deposition process when only the gas-phase density of the species is known.

Methods that have been applied to determine the surface reaction probability of plasma radicals include time-resolved measurements of the radical density in pulsed plasmas[7,8] and the measurement of spatial concentration profiles near reactor walls.[9,10] The extraction of the surface reaction probability from these data generally requires extensive modeling of the diffusional transport equations for the plasma.[11] One method that requires fewer assumptions and for which the interpretation of the data is more straightforward is the imaging of radicals interacting with surfaces (IRIS) technique. With this method, the surface reactivity of radicals *during* plasma processing is directly measured by two-dimensional imaging using laser-induced fluorescence (LIF). Furthermore, this method enables the exploration of the dependence of the surface reactivity on plasma parameters, substrate material, substrate temperature, and ion bombardment, because the use of a molecular beam facilitates independent variations of the plasma and surface conditions. Moreover, with IRIS even the determination of the surface reactivity of radicals whose loss is dominated by gas-phase collisions rather than by surface reactions is straightforward.

An IRIS experiment has previously been used to study the surface reactivity of a number of radicals in several plasma systems, including the reactivity of SiH in SiH_4 plasmas. Early IRIS studies by Ho et al.[12] focused on SiH measurements using

* To whom correspondence should be addressed. E-mail: erfisher@lamar.colostate.edu.
[†] E-mail: wmmkessels@tue.nl.
[‡] Current address: LSI Logic, Troutdale OR.
[§] Current address: Mattson Technology, Inc., 3550 W. Warren Avenue, Fremont, CA.

10.1021/jp013895q CCC: $22.00
Published on Web 02/09/2002

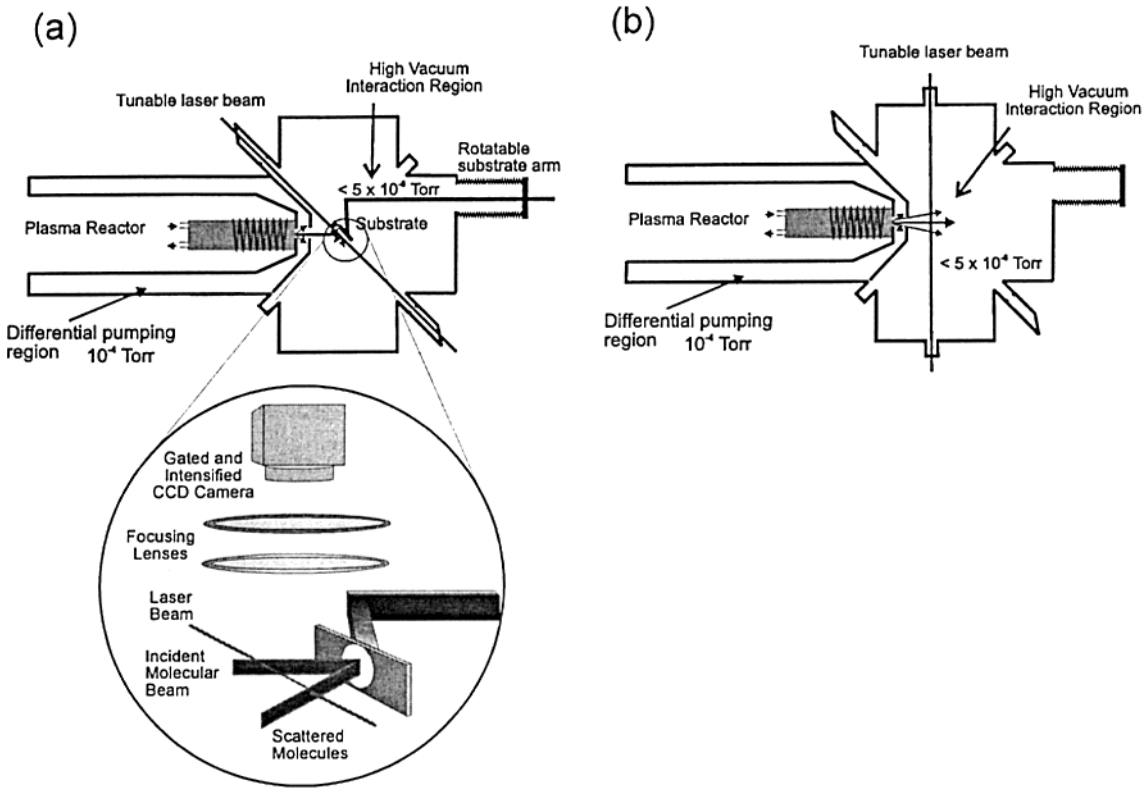

Figure 1. Top view of the IRIS apparatus in two configurations (a) for surface reactivity measurements and (b) for velocity measurements. In part a, the interaction region of the molecular beam with the substrate (for specular scattering of the beam) and the collection optics are given in detail.

SiH_4 plasmas with a limited set of experimental conditions and found a high surface reaction probability, 0.94 ± 0.05. Likewise, later IRIS measurements of SiH by McCurdy et al.[13] utilized SiH_4 plasmas and examined the substrate temperature dependence of the reactivity. This study also found a high surface reaction probability of 0.95 ± 0.05, with no discernible dependence on substrate temperature. In the present work, the surface reactivity of SiH using various plasma sources (SiH_4, Si_2H_6, SiH_4/H_2, Si_2H_6/H_2, SiH_4/NH_3, SiH_4/N_2, SiH_4/CH_4) will be considered. Specifically, we have examined whether the SiH surface reactivity changes with material being deposited and whether the determined values of the surface reactivity approximate the previously found high surface reactivity of SiH on a-Si:H. These data provide information on the surface reactions of SiH during deposition of silicon-based materials and can be directly compared to recent molecular dynamics (MD) simulations of SiH surface interactions.

In addition to the surface reactivity measurements, the present work also addresses the power dissipation in SiH_4 and Si_2H_6 plasmas by specifically examining the energetics of SiH production. The study of these aspects of plasma chemistry is important for elucidation of mechanistic details for plasma deposition of silicon-based materials; however, the energy distributions of radicals in plasmas are usually difficult to determine. Schmitt et al. have performed an extensive study on SiH, concentrating primarily on the rotational heating and collisional relaxation of SiH produced from SiH_4 by electron impact.[14] These experiments were performed by time-resolved LIF measurements in the postdischarge of a dc multipole SiH_4 plasma, and the data are used for comparison to the present results with two caveats. First, as noted by Schmitt et al., the measurements were fairly inaccurate for the kinetic translational temperature of SiH, and several assumptions were made in deriving the value. Second, the experiments in the dc discharge with 70 eV electrons are not necessarily a good approximation for the commonly applied rf SiH_4 processing plasmas.

The IRIS experiment yields the opportunity to study both the kinetic translational temperature (Θ_T) and the rotational temperature (Θ_R) of radicals in an rf excited plasma with relatively high accuracy.[15−17] The average kinetic translational temperature can be determined by taking two-dimensional "snapshots" of the LIF intensity for different time delays after the laser excitation of the SiH radicals in the molecular beam. Evaluation of the velocity profiles leads to Θ_T. Θ_R is determined by measuring a portion of the silylidyne radical's LIF excitation spectrum. These experiments provide valuable information on the relationship between the kinetic and rotational temperature of radicals in processing plasmas. This is useful because temperature considerations in these plasmas are often based on measurements of only one of these temperatures,[18] which may not be an accurate representation of the true values. Similar IRIS measurements for NH_2 in NH_3 plasmas[13] and OH in tetraethoxysilane/O_2 plasmas[16] have revealed important information on the power dissipation in these plasmas and on the creation mechanism of the radicals.

II. Experiment

A. IRIS Apparatus. The IRIS apparatus (Figure 1) for reactivity and velocity measurements has been described in detail previously.[13,15] In a typical IRIS experiment, an inductively coupled plasma is created in a glass reactor, after which the plasma is expanded into a double differentially pumped high-vacuum chamber. This generates a near-effusive molecular beam consisting of virtually all species present in the plasma. Using spatially and temporally resolved LIF allows the study of either the interaction of the radicals with surfaces (Figure 1a) or the velocity of the radicals in the molecular beam (Figure 1b). For reactivity measurements, the LIF intensity of a freely expanding

molecular beam is compared with the LIF intensity of a molecular beam that is directed onto a substrate. The difference in LIF intensity is directly proportional to the amount of radicals scattered and/or created at the substrate's surface. In the velocity measurements, "snapshots" of the LIF intensity of a freely expanding molecular beam are taken at different delays after the laser excitation pulse. The velocity of the radicals can subsequently be deduced from the spatial shift in maximum intensity of the fluorescence between the different delays.

The plasma is produced by the inductive coupling of 13.56 MHz rf power (5−100 W) to an eight-loop induction coil surrounding the glass plasma reactor and tuned by a variable capacitor matching network. Plasmas are created in 100% SiH_4 (Matheson 99.999%) and 100% Si_2H_6 (Voltaix 99.99%) and in SiH_4 mixtures with H_2 and N_2 (both Air Products 99.999%) and NH_3 and CH_4 (both Air Products 99.99%). With mixtures, the gases are premixed before entering the reactor. The total gas flow is typically maintained at 10−20 sccm (standard cm^3 per minute) leading to source pressures of 30−60 mTorr. This pressure range together with the relatively high powers leads to primarily inductive coupling of the plasma. Therefore, no transition from the α-regime to the γ-regime is expected,[19] contrary to the results of Scott et al.,[20] who had essentially capacitive coupling in a similar "inductively coupled" plasma.[21]

The expansion of the plasma into the first differentially pumped region takes place through a 5 or 10 mm diameter orifice leading to a typical pressure of $\sim 5 \times 10^{-4}$ Torr in this region. The molecular beam is subsequently collimated by two 1.0 mm wide slits (located at 38 and 50 mm from the orifice) when entering the second differentially pumped region. The pressure in this vacuum chamber is typically $\sim 10^{-5}$ Torr during plasma operation. The mean free path for momentum transfer of SiH in the SiH_4/Si_2H_6 environment of the plasma reactor is ∼4 mm for the typical conditions used, as calculated from the Lennard-Jones parameters for SiH, SiH_4, and Si_2H_6.[19] Considering the dimensions of the gas extraction orifice (5−10 mm) and the slit widths (1 mm), this means that the molecular beam in the high vacuum chamber is best classified as collisionless "near-effusive".[22]

Laser radiation is produced at ∼414 nm for probing the SiH $A\ ^2\Delta \leftarrow X\ ^2\Pi$ transition (Figure 2). This is achieved by pumping a dye laser (Lambda Physik, Scanmate 2) with a 308 nm XeCl excimer laser (Lambda Physik LPX210i, 100 mJ, 17 ns, 100 Hz). Two different dyes were used for the experiments described. The first dye, Furan 2 (Lambda Physik), was used to probe the R_{21} ($J = 1.5$) rotational line at 411.542 nm with a typical laser energy of 2−6 mJ/pulse. The second dye, Excalite 417 (Exciton), allowed access to the R_{12} ($J = 1.5$) rotational line at 414.434 nm as well as the Q_1 ($J = 10.5$) and R_2 ($J = 2.5$) rotational lines at 413.418 and 413.428 nm, respectively. With this dye, the laser energy is typically 1−3 mJ/pulse. A lens is used to focus the laser radiation at the position of the molecular beam, yielding a well-defined laser beam <1 mm wide. Measurements of the fluorescence signal as a function of the laser energy yielded typical optical saturation behavior for the transitions investigated. All reactivity and velocity experiments were performed at energies in the optical saturation regime such that the measurements are not affected by small fluctuations in laser power.

Total fluorescence is detected by an intensified charge-coupled device (ICCD, Princeton Instruments) located perpendicular to both the molecular beam and the laser beam, directly above the interaction region. The ICCD is electronically gated with respect to the trigger of the laser pulse ("gate delay"), and signal is collected during the "gate width". SiH fluorescence is collected by a set of two lenses, with focal lengths of 300 and 75 mm, imaging a 2030 mm^2 area onto the 586 × 384 pixel array of the ICCD.

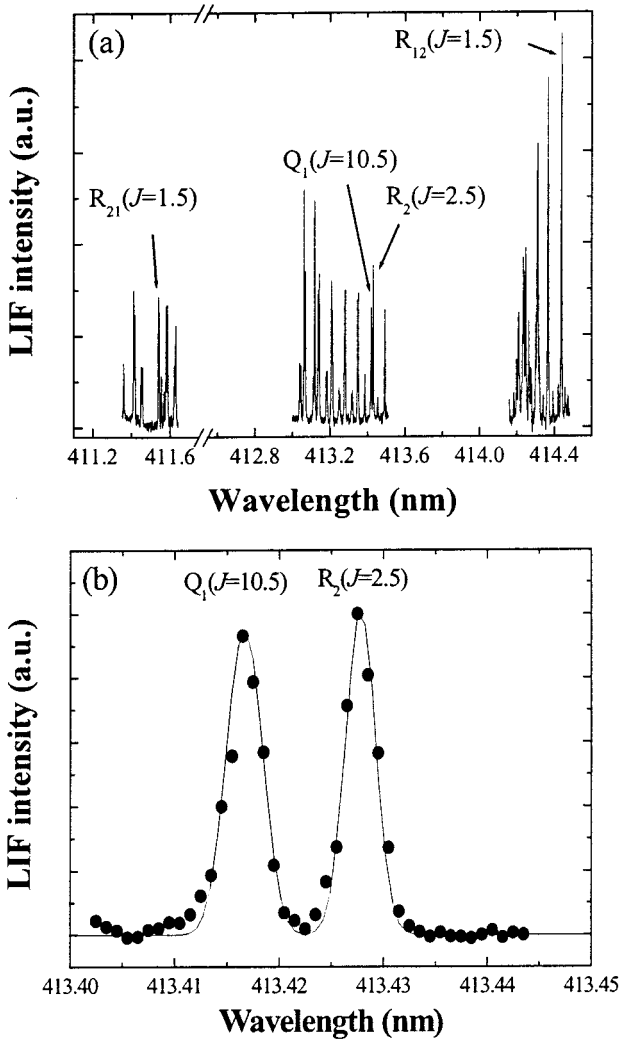

Figure 2. (a) The SiH $A\ ^2\Delta \leftarrow X\ ^2\Pi$ excitation spectrum from 411 to 415.6 nm obtained with the Excalite 417 dye and a 100% SiH_4 plasma. The spectrum is not corrected for variations in laser power. The rotational lines probed in the IRIS reactivity experiments are indicated. (b) The portion of the spectrum used for determining the SiH rotational temperature together with the simulated spectrum. In both figures, the Lambda doubling of the rotational lines is not resolved because of optical saturation of the transition.

B. Reactivity Measurements. For reactivity measurements (Figure 1a), the laser radiation is directed into the chamber such that it intersects the molecular beam at a 45° angle. A substrate (10 × 40 mm^2 p-type Si wafer with native oxide) can be rotated into the path of the molecular beam with its surface parallel to the laser beam. The laser−surface distance is maintained within the range of 2−5 mm. Every reactivity experiment consists of a set of four measurements: one with the substrate rotated in and one with the substrate rotated out of the molecular beam while probing a SiH rotational line ("on resonance"), and the same two measurements at an off-resonance, or background, laser wavelength. Each measurement consists of five accumulations of 6000 laser shots, and the final reported reactivity values are the average of four separate reactivity experiments. During reactivity measurements, the pixels of the ICCD are 4 × 4 binned and the gate delay is typically 80 ns with respect to the laser excitation of SiH. The gate width is typically 2000 ns such

that the fluorescence is collected over the entire radiative lifetime of the SiH $A^2\Delta$ state (534 ns).[27] For the determination of the SiH surface reaction probability, the "off-resonance" images are first subtracted from the "on-resonance" images to correct for spurious signals due to plasma emission and possible scattered laser light. Subsequently, the image with no substrate is subtracted from the image with the substrate, yielding the possible scatter and/or production of SiH at the substrate surface. Finally, the two-dimensional images of the freely expanding molecular beam (i.e., the final image for substrate out) and surface scatter are converted into one-dimensional cross-sectional plots by averaging over 10 rows of pixels (3.8 mm wide) along the laser axis.

To extract the surface reactivity of the radicals, the numerical simulations described previously[12,16] are used to model the cross sectional data. Briefly, the spatial distribution of the radical number density along the laser beam is calculated for radicals in the molecular beam and for those scattered at the surface based on the known geometry of the experiment. In the simulations, all incident radicals scatter from the surface (i.e., zero surface reaction probability) with an assumed cosine distribution about the surface normal.[24] The resulting simulated curve for the scattered radicals is compared to the corresponding experimental data, and the radical's surface reaction probability is derived from the scaling factor S necessary to match the experimental data. A value of $S < 1$ means that radicals are lost at the surface with a surface reaction probability $R = 1 - S$, whereas $S > 1$ indicates surface production of the radical species.

There are four issues that need to be addressed associated with using the IRIS method for measuring surface reactivities of radicals. First, surface reactivity measurements are performed by probing a single rotational state, whereas the surface reaction probability of molecules and radicals can be rotational state dependent.[25] In this and previous work,[10,12] however, no difference in surface reactivity has been observed with different rotational states of SiH or for other radicals. A second, related issue is that the rotational state of SiH can change after interacting with the substrate as a result of thermal equilibration on the surface. This might require a correction to the scatter values, S, to account for differences in rotational state populations as IRIS experiments only consider one rotational state for each measurement.[16,17] Measurements are, however, performed on SiH states with low rotational quantum numbers and, therefore, this correction is negligible, even when complete thermal equilibration of the incident radicals with a typical Θ_R of ~600 K (see section III.B) at the substrate (300 K) is assumed. Third, in the simulation procedure, the surface reactivity is determined from the density of the radicals in the incident beam and scattered signals, whereas the flux of incident and scattered radicals should be considered.[17] Using the velocity of SiH in the incident molecular beam as presented in section III.B and assuming a velocity of the scattered SiH corresponding to full thermal equilibration at the surface, a possible correction for the surface reaction probability of SiH in the present work is small compared to the experimental error. The final issue that needs to be considered is the Doppler shift induced by the geometry of the IRIS experiment.[16,17,26] The laser wavelength is optimized for maximum signal for the incident molecular beam, thereby possibly discriminating against scattered radicals that may have slightly different optimum wavelengths because of different velocity distributions, both in magnitude and direction of the velocity. For the SiH rotational lines probed, no detectable shift in wavelength for maximum signal intensity has been observed. Moreover, this has been explicitly examined previously for NH and OH radicals.[12,27]

C. Velocity and Temperature Measurements. The random kinetic velocity of a radical corresponding to the radical's average kinetic translational temperature in the bulk of the plasma can be determined by measurements of the velocity of the radical in a molecular beam effusively extracted from the plasma. In IRIS experiments, the gas extraction is nearly effusive. This means that the velocity of SiH in this molecular beam approximates the random velocity of SiH in the plasma and that this can be used to study the kinetic translational temperature of SiH in the plasma.

For velocity measurements, the laser is directed into the high vacuum chamber such that it intersects the molecular beam at a 90° angle (Figure 1b). This leads to a better spatial resolution of these measurements compared to that afforded by the 45° angle used in reactivity experiments. To further improve spatial resolution, the ICCD pixels are not binned for velocity measurements. ICCD images are collected for different gate delays (typically 65, 565, 1065, and 1565 ns after the laser pulse for SiH excitation) and with a narrow gate width of 100 ns. At each gate delay, the LIF signal is collected over four accumulations of 60 000 laser shots. The two-dimensional images are converted into one-dimensional cross-sectional plots by averaging over 50 rows of pixels (4.75 mm wide) along the central axis of the molecular beam. This leads to "snapshots" of the spatial position of the LIF intensity at the different gate delays.

To extract the velocity of SiH from these measurements, a slightly different approach was used than has been previously reported.[13,16] First, the position of the maximum LIF intensity at every gate delay is determined from the cross-sectional plots assuming a symmetrical laser spatial profile. These maxima are plotted as a function of gate delay and fit with a linear regression. The slope of this linear fit corresponds to the average velocity of SiH along the molecular beam's central axis. This is a lower limit of the velocity of SiH, because the molecular beam also expands in the radial direction. Subsequently, the spatial LIF intensity of SiH along the molecular beam's central axis is simulated as a function of the gate delay for different kinetic temperatures. This is done using a Monte Carlo simulation program,[13,16] which assumes that the velocity distribution in the plasma is described by the Maxwell−Boltzmann distribution. The peak maxima of the simulated data are then analyzed as described above. Comparison of the experimentally obtained value with the simulated values is performed in an iterative fashion, yielding the velocity and, thereby, Θ_T of SiH in the plasma. The result of this procedure does not differ from the previously reported method (i.e., fitting the simulated profiles to the experimental profiles by optimizing Θ_T); however, this method is very straightforward and is more sensitive to small spatial changes in the LIF signal. This is especially important in the present work, because SiH has a relative short lifetime compared with the radicals previously investigated.[13,16] This results in a much more limited range of gate delays that can be accessed, yielding a very small spatial displacement of SiH per step in gate delay.

The rotational temperature of SiH is deduced from the relative height of the neighboring Q_1 ($J = 10.5$) and R_2 ($J = 2.5$) rotational lines at 413.418 and 413.428 nm (Figure 2b). This relationship is sensitive to Θ_R, because of the relatively large difference in rotational quantum number. Both lines are scanned in an excitation LIF spectrum with a step size of 0.001 nm in wavelength, and LIF signal is collected for 3000 laser shots per step. For these experiments, the ICCD was 4 × 4 binned,

TABLE 1: Surface Reaction Probability of SiH in Various Silane-Based Plasmas[a]

source gases	flow ratio	R
SiH_4		0.95(0.05)[b]
		>0.94[c]
Si_2H_6		0.95(0.03)
SiH_4/H_2	1:5 and 1:10	0.95(0.07)
Si_2H_6/H_2	1:5 and 1:10	0.95(0.07)
SiH_4/NH_3	1:1.33	0.98(0.05)
SiH_4/N_2	3:1	0.97(0.03)
SiH_4/CH_4	1:1	0.96(0.07)

[a] The substrate temperature is 300 K, unless otherwise stated. The errors for the surface reaction probability are in parentheses. Unless otherwise noted, all *R* values are results from the present work. These values correspond to β values cited elsewhere. [b] Value is from ref 13 and is independent of substrate temperature between 300 and 673 K. [c] Value is from ref 12, for IRIS studies of SiH on a-Si:H at 300 K.

the gate delay with respect to SiH excitation is ~80 ns, and the gate width is 2000 ns. Θ_R is ultimately determined from simulations of the SiH rotational lines using the program LIFBASE, an example of which is shown in Figure 2b.[28]

III. Results and Discussion

A. Reactivity Measurements. The surface reactivity of SiH has been measured for several SiH_4- and Si_2H_6-containing plasmas used for the deposition of the silicon-based materials a-Si:H, μc-Si:H, a-SiN_x:H, and a-SiC_x:H. The plasmas used and *R* values measured for SiH are listed in Table 1. The substrate temperature was 300 K for all measurements made in gas mixtures. As noted in Table 1, the previously reported IRIS data for SiH on a-Si:H using SiH_4 as the source gas showed no dependence on substrate temperature.[13] For the gas mixtures, the conditions were chosen such that the SiH_4 was highly diluted while a sufficient S/N ratio was maintained for the SiH LIF collection. For each gas mixture, data were taken for two different plasma powers (~30 and ~60 W). Within experimental accuracy, however, no dependence on plasma power was observed. Thus, the reported values for *R* have been averaged over the two different powers. Furthermore, for all gas mixtures, no transitions in the excitation spectra were observed other than those belonging to the SiH A $^2\Delta \leftarrow$ X $^2\Pi$ transition. More specifically, no traces of the SiN B $^2\Sigma \leftarrow$ X $^2\Sigma$ transition, which lies in the same wavelength range as that of SiH, were observed in the excitation spectrum for the SiH_4/NH_3 and SiH_4/N_2 plasmas.[29,30]

As can be seen from Table 1, the surface reaction probability of SiH is nearly unity, not only for the previously studied SiH on a-Si:H system[12,13] but also for SiH on the other deposited materials. Figures 3 and 4 show a typical example of IRIS data for SiH using the SiH_4/CH_4 plasma. From the images in Figure 3, it is evident that the magnitude of the signal from scattered radicals is much lower than that for SiH radicals in the incident molecular beam. SiH has therefore a very low probability of surface scattering, if any. Indeed, the scattered SiH signal (Figure 4) is just slightly higher than the noise level and displays a cosine behavior as evidenced by the reasonable fit to the simulation. The cosine distribution does not necessarily mean that incident SiH radicals reside on the surface for a short time before desorbing.[12] It can also imply that all SiH is lost at the surface but that some other process (e.g., ion bombardment) leads to a small surface production of SiH. The IRIS experiment does not, however, distinguish between these two processes. Notwithstanding, SiH has a near-unity surface reaction probability that is independent of substrate temperature (for at least a-Si:H), plasma conditions, and film composition for the conditions and materials studied here.

As also indicated by the results of previous IRIS studies,[12,13] the very high surface reaction probability of SiH is probably inherent to the nature of the radical itself, as it is independent of substrate temperature and film composition. For a-Si:H films, the surface reaction probability of SiH is much higher than for the radicals SiH_3 and SiH_2,[7,31] for example, and it is also higher than the surface reaction probability of SiH_2 on a-SiC_x:H.[32] These observations, combined with recent molecular dynamics (MD) simulations, provide insight on the reactions of SiH as well as SiH_2 and SiH_3 species during film growth. Ramalingam et al. have studied the radical−surface interactions for a-Si:H film growth by MD simulations for SiH_3, SiH_2, and SiH molecules.[33−36] In these simulations, the surface reaction probability of the radicals was investigated and generally good agreement with experimental data from the literature was found.[31,33−36] For SiH, a surface reaction probability of 0.95 on a 300 K a-Si:H film was determined from 25 separate simulations.[33,34] Interestingly, in all cases in which SiH was lost to the surface, the SiH contributed to the film growth and no other reactions were observed. This strongly suggests that the values for the surface reaction probability reported in Table 1 are the actual sticking probabilities of SiH on the different types of films.

Radical "sticking" is one type of reaction in which the radical is lost at the surface. In addition to sticking, surface loss of radicals can also occur via abstraction of a surface atom or recombination with another radical at the surface. The MD simulations have shown, however, that for a-Si:H growth, SiH only sticks to the dangling bond reactive sites on the film, whereas insertion into surface Si−H bonds does not occur. These insertion reactions have been proposed[37,38] on the basis of the analogy with gas-phase reactions of SiH and SiH_2 radicals with SiH_4.[39] According to the MD simulations, the composition of the film and surface strongly affects the nature of the SiH sticking reaction, but not the sticking probability. There is not only a large difference between reactions on a-Si:H when compared to both hydrogenated and pristine, crystalline silicon surfaces, but there are also important differences between a-Si:H films with different properties.[33,34] For a-Si:H films with a reasonably high surface dangling bond density, sticking of the incident SiH occurs almost directly when the radical arrives at the surface. For more hydrogenated surfaces, the SiH radical migrates short distances on the surface until it finds a dangling bond; whereas on fully hydrogenated a-Si:H surfaces the SiH penetrates into the a-Si:H bulk. In the bulk, the SiH attaches itself to dangling bonds, which are typically present in nanoscopic cavities that emanate from the surface of the film. Furthermore, the simulations suggest that the sticking probability of SiH depends on the orientation of the impinging SiH radical. As expected, the SiH radical is less reactive with the film when the radical approaches the surface in a H-down configuration. For a-Si:H, however, the SiH radical tends to orient itself in the Si-down configuration as it approaches the surface.[33,34]

These types of reactions involving SiH during a-Si:H growth are likely valid for the other Si-based materials investigated here. In particular, the observation that SiH only sticks by attaching itself to a dangling bond makes these reactions more general, because the insertion reaction into Si−H bonds would depend strongly on the Si−H surface coverage. The chemical nature of a-Si:H surfaces is expected to be different for Si alloys such as a-SiN_x:H and a-SiC_x:H than for a-Si:H and μc-Si:H. Thus, SiH can play an important role in the deposition process and

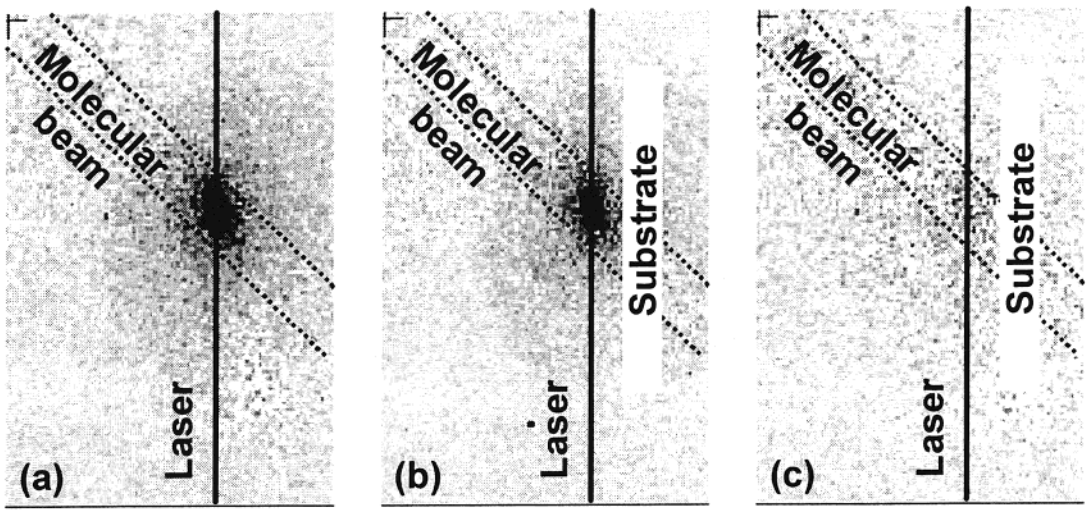

Figure 3. Spatially resolved two-dimensional ICCD images of LIF signals produced by SiH radicals in a SiH_4/CH_4 plasma (10 sccm SiH_4, 10 sccm CH_4, ~60 mTorr, 67 W applied rf power). In part a, the molecular beam is freely expanding, whereas in part b, an a-Si:H covered Si substrate (300 K) is in the path of the molecular beam. The image shown in part c is the difference between the images shown in panels a and b, corresponding to SiH radicals scattering from the substrate. Darker regions in the images correspond to higher SiH LIF intensities. The laser−substrate distance is 4 mm, and the displayed area in each image is 55.6 × 36.5 mm^2.

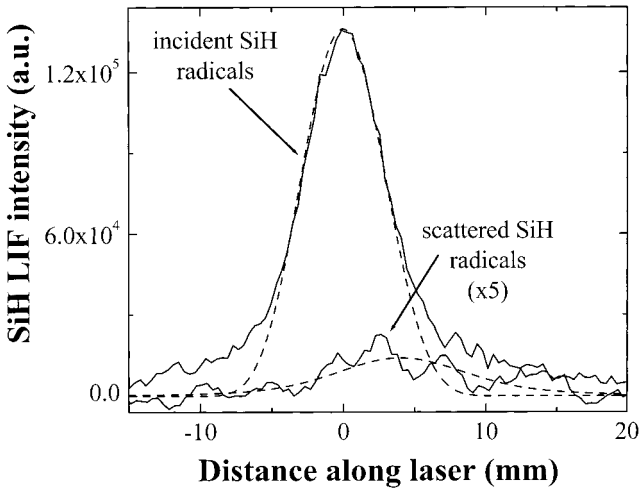

Figure 4. Cross-sectional data of the SiH IRIS images presented in Figure 3. LIF signals are shown for radicals in the molecular beam incident on the substrate and for radicals scattering from the substrate (corresponding to parts a and c of Figure 3, respectively). An average of four separate data sets is shown and the magnitude of the scattered radicals is multiplied by a factor of 5 for clarity. Dashed lines are simulated curves as obtained by the reactivity simulation code described in the text, yielding $S = 0.02 \pm 0.03$. This corresponds with a surface reaction probability for SiH on a-SiC_x:H of $R = 0.98 \pm 0.03$.

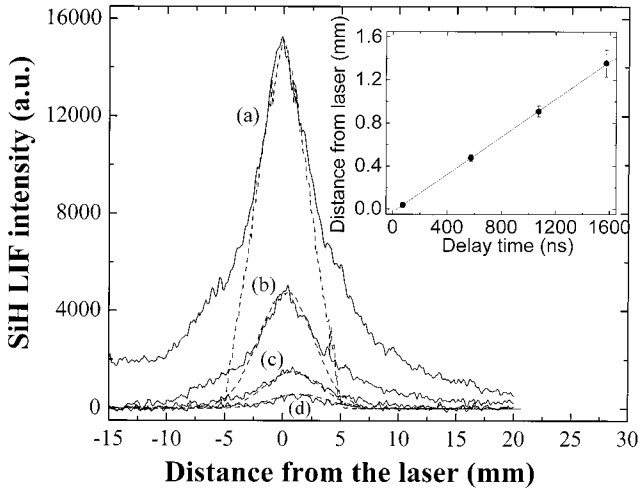

Figure 5. Cross-sectional images of the "snapshots" of the SiH fluorescence in a SiH_4 plasma (20 sccm SiH_4, ~35 mTorr, 61 W applied rf power) at four different gate delays: (a) 74 ns, (b) 574 ns, (c) 1074 ns, and (d) 1574 ns after laser excitation of the SiH in the chamber. Simulated curves using the velocity simulation code as described in the text for a kinetic SiH temperature of 1058 K are also shown (dashed lines). In the inset, the spatial positions of the maximums of the LIF signals are plotted as a function of gate delay. The slope of the linear fit corresponds to the velocity of the SiH radicals along the central axis of the molecular beam, a lower limit to the SiH velocity in the molecular beam.

film properties of the studied materials. Although the SiH density is usually relatively low in SiH_4 plasmas,[40−43] this low density is partially compensated by the very high sticking probability of the radical. Furthermore, the electronic properties of the materials, which are very sensitive to defect concentrations in the films, can be determined to a large extent by the minority species in the plasma. As directly observed in the MD simulations,[33,34] SiH radicals introduce dangling and floating bonds in the film. For plasma conditions with a relatively high SiH density, the high surface reactivity of SiH and the subsequent introduction of dangling bonds leads to almost random film growth and a high surface roughness, ultimately resulting in low film density and poor structural film properties.[44,45]

B. Velocity and Temperature Measurements. SiH velocity measurements have been made for 100% SiH_4 and 100% Si_2H_6 plasmas as a function of the applied rf plasma power. For these experiments, the gas flows for SiH_4 and Si_2H_6 were 20 and 10 sccm, leading to source pressures of ~ 45 and 35 mTorr, respectively. A typical SiH velocity measurement is shown in Figure 5 for a 100% SiH_4 plasma at an applied plasma power of 61 W. The cross-sectional images have been extracted from the two-dimensional "snapshots" of the LIF intensity measured at different gate delays after laser excitation of SiH (100 ns gate width). The data clearly show that the position of the LIF intensity shifts away from the laser as the gate delay increases (at the shortest gate delay the LIF intensity peaks at essentially zero distance from the laser). This shift is more apparent in the inset of Figure 5, which shows the position of maximum LIF intensity as a function of the gate delay. The data points in the

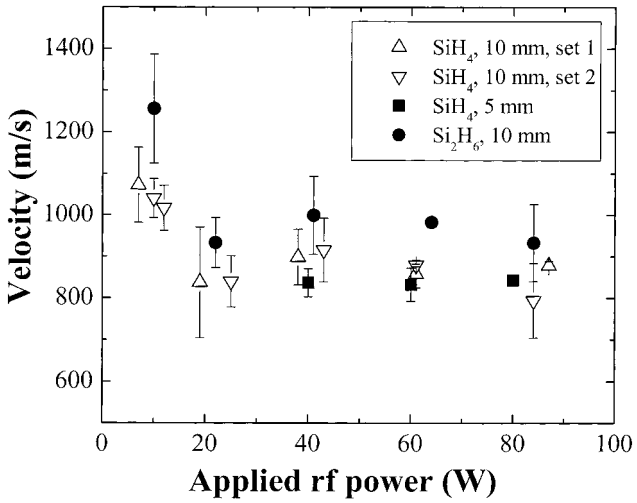

Figure 6. Velocity of SiH in the molecular beam as a function of applied rf power for SiH in SiH_4 and Si_2H_6 plasmas. For SiH_4, results from three separate data sets are shown. The first two were obtained using a plasma extraction orifice of 10 mm, with an intermediate time interval of ~2 months, and the third set was obtained using a 5 mm extraction orifice, ~3 months after the second data set.

inset are well-described with a linear regression analysis, demonstrating that the velocity of SiH in the molecular beam is constant with no acceleration or deceleration. Another observation is that the SiH LIF intensity decreases for increasing gate delays. This is caused by depopulation of the excited SiH $A^2\Delta$ state by radiative decay after the laser excitation pulse. The steps in gate delay (500 ns) are nearly as long as the 534 ns radiative lifetime of the SiH A $^2\Delta$ state. To obtain a high accuracy for the measurements, data is preferentially taken up to very high gate delays, but this is obviously limited by the remaining LIF intensity.

As noted above, the slope of the linear fit in the inset of Figure 5 yields a lower limit of the average SiH velocity in the molecular beam, because it corresponds to the velocity along the molecular beam axis while there is also expansion of the beam in the radial direction. This lower limit of the velocity has been used as a starting point in the simulations to obtain the average SiH kinetic velocity v_{kin} in the plasma and the corresponding average kinetic translational temperature, Θ_T ($\Theta_T = \pi m v_{kin}^2/8k$, with m being the mass of the radical and k being Boltzmann's constant). Cross-sectional images of the SiH LIF intensity have been simulated for different kinetic velocities and temperatures using different time delays. Using a similar analysis, the simulations were iteratively compared with the experimental cross-sectional data until good agreement between experiment and simulation was obtained. The simulated cross-sectional data are also shown in Figure 5. Although the agreement between the experimental and simulated cross-sections is good for the central part of the SiH distribution (center of laser beam), the "wings" of the distribution are clearly not well described by the simulation. This discrepancy is likely caused by the laser spatial intensity profile deviating slightly from the ideal Gaussian distribution,[13] which does not affect the determined kinetic velocity and temperature. For the data in Figure 5, the simulation procedure yields an average kinetic velocity of 879 ± 3 m/s and, correspondingly, $\Theta_T = 1058 \pm 8$ K. The experimental error in these values is determined from the standard deviation in the linear regression analysis of the maximum LIF intensity versus delay.

In Figure 6, the average kinetic velocity of SiH in the SiH_4 and Si_2H_6 plasmas is shown as a function of the applied rf power. Three data sets, obtained over a 5 month time period, are shown for the SiH_4 plasmas, indicating good reproducibility of the velocity measurements. One of these data sets was acquired using a smaller extraction orifice (5 mm vs 10 mm for the other two data sets) for the plasma source. As shown in Figure 6, there is no significant difference in velocity measured for molecular beams formed using two different orifice diameters, as expected for an effusive or nearly effusive molecular beam.[22] This demonstrates that Θ_T of SiH in the plasma can be measured from the velocity of SiH in the molecular beam extracted from the plasma. Note that the SiH velocities and temperatures measured with the Si_2H_6 plasma are only slightly higher than those measured in the SiH_4 plasmas at all applied rf powers.

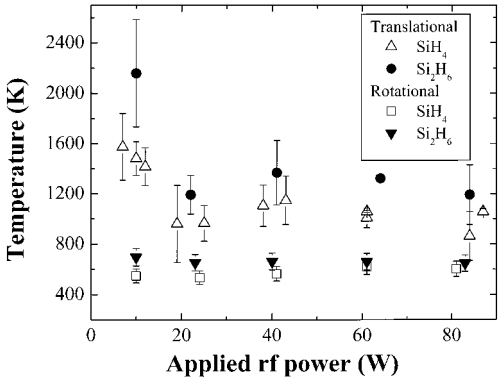

Figure 7. Average kinetic temperature, Θ_T, and rotational temperature, Θ_R, of SiH in SiH_4 and Si_2H_6 plasmas. The Θ_T values correspond to the velocities given in Figure 5.

The average SiH kinetic translational temperatures are given as a function of applied rf power in Figure 7. The values measured for SiH are relatively high, ~1100−1200 K, and are nearly independent of the applied power. At very low plasma powers, however, Θ_T values are significantly higher than the values measured at all other rf powers. This is most likely the result of plasma instabilities associated with the difficulty in sustaining the plasma at these low powers. Under other circumstances where the plasma was very unstable (e.g., due to the presence of a very thick a-Si:H coating on the reactor walls), very high kinetic velocities and temperatures have also been measured. At rf powers of ≥20 W, the kinetic velocity of SiH is essentially independent of the applied rf power for both SiH_4 and Si_2H_6 plasmas.

Figure 7 also shows Θ_R of SiH as determined from two closely spaced rotational lines with considerably different quantum numbers (Figure 2b). Θ_R is also roughly independent of the applied rf power, although it shows a slight increase with power for the SiH_4 plasma. The rotational temperatures are roughly equal for the SiH_4 and Si_2H_6 plasmas, and the data show a good agreement with the previously determined $\Theta_R = 600 \pm 40$ K measured with a different IRIS apparatus (30 W, 15 mTorr SiH_4).[12] The most striking observation is that Θ_R for SiH, ~600 K, is much lower than Θ_T for SiH, ~1200 K.

The observation that Θ_R and Θ_T of SiH are roughly independent of the applied rf power indicates that increasing the rf power does not lead to kinetic or rotational heating of the SiH radicals. In Figure 8, the total SiH LIF intensities for both the SiH_4 and Si_2H_6 plasmas are given as a function of the applied plasma power. The figure shows that the LIF intensity increases drastically at low powers and more gradually at higher powers. This indicates that SiH_4 and Si_2H_6 dissociation increases with increasing rf power and, therefore, that when going to

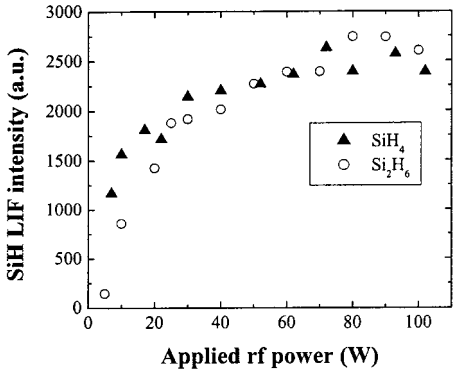

Figure 8. Total SiH LIF intensity in arbitrary units for the SiH_4 and Si_2H_6 plasma as a function of the rf applied power.

higher powers, a portion of the energy dissipated is used for SiH_4 and Si_2H_6 dissociation.

To address the power dissipation and the observed SiH temperatures in the inductively coupled plasma, first consider the creation mechanism of SiH in SiH_4 and Si_2H_6 plasmas. In the SiH_4 plasma, SiH is created primarily directly by electron-induced dissociation of SiH_4, reaction 1,[19]

$$e^- + SiH_4 \rightarrow SiH + H + H_2 + e^- \qquad (1)$$

rather than via a sequential dissociation of SiH_3 or SiH_2,[46] as shown in reaction 2,

$$SiH_x\,(x = 2, 3) + e^- \rightarrow SiH + H\,(H_2) + e^- \qquad (2)$$

Reaction 1 proceeds via superexcited electronic transient states of SiH_4 and accounts for ~12% of the SiH_4 dissociation process.[15] In Si_2H_6 plasmas, however, SiH is not an important direct reaction product[19] but is likely created through dissociation of SiH_4. The SiH_4 density is generally very high in Si_2H_6 plasmas as a result of gas-phase reactions and radical recombination at the reactor walls that lead primarily to SiH_4.[47] This can also explain the similarity in the Θ_T and Θ_R values we have measured for SiH in SiH_4 and Si_2H_6 plasmas.

As noted in the Introduction, Schmitt et al. studied SiH radicals created by electron-induced dissociation of SiH_4.[14] In this seminal work, time-resolved rotational temperature measurements were made on SiH in SiH_4 and SiH_4/H_2 postdischarges in a dc multipole reactor. It was found that SiH is created in a high degree of rotational excitation and that Θ_R decreases from 950 K initially to the 500 K gas temperature at a later time in the afterglow. A corresponding rotational relaxation rate (cooling rate) of 1.5×10^{-10} cm^3/s was determined for SiH radicals in the X $^2\Pi$ state. Schmitt et al. also determined Θ_T of SiH, albeit with relatively poor accuracy. They observed an initial Θ_T of 800 ± 200 K, which is again higher than the background gas temperature.

These initially higher rotational and kinetic translational temperatures of SiH can be explained by heating of the created SiH radicals by the excess energy released in the electron-induced dissociation of superexcited SiH_4. This excess energy, approximately the electron energy less the SiH_4 dissociation energy, is carried away by the dissociation products. Most of the energy is carried away by the lighter fragments (i.e., hydrogen), but part of the energy is stored in the translational and rotational degrees of freedom of the SiH. This leads to SiH temperatures that are initially higher than the ambient gas temperature. Collisions with other plasma species eventually lead to relaxation of the temperatures to the gas temperature.

The rotational relaxation rate determined by Schmitt et al. indicates that the probability for rotational−rotational and rotational−translational transfer in molecular collisions is almost unity (compare the relaxation rate with the SiH collisional rate with SiH_4 of $\sim 3 \times 10^{-10}$ cm^3/s at 500−1000 K).[19] This high probability is usually explained in terms of the observation that the energy associated with Θ_T is, at typical plasma operating temperatures, on the order of the energy separation between the rotational levels of SiH and SiH_4. These types of considerations are also the basis for the commonly applied assumption that the average rotational temperature of the gas-phase species (including stable species such as SiH_4 as well as transient species such as radicals) is equal to their average kinetic translational temperature and thus to the ambient gas temperature. The gas temperature is, therefore, often derived from the rotational temperature of a single species such as SiH, which is easily determined from emission or absorption measurements.[7,18,19,43]

The results presented here are apparently not in agreement with these assumptions, because Θ_T is considerably higher than Θ_R for SiH in the plasma. On the other hand, the observation that the temperatures are roughly independent of the applied rf plasma power would suggest that the SiH temperatures are determined by the creation mechanism of SiH via electron-induced dissociation of SiH_4 (Si_2H_6) (reaction 1). The energetics of this creation mechanism should be nearly independent of the plasma power. On the basis of the rotational relaxation rate, we expect that the rotational temperature of SiH is thermalized to the average gas temperature before the SiH is extracted from the plasma. Thus, we believe the gas temperature is ~600 K. It should be noted, however, that SiH has a rather high reactivity with SiH_4 to produce higher order silanes and radicals and that the SiH probed must have been created relatively close to the extraction orifice. Using the reaction rate of SiH with SiH_4,[39] we estimate that a SiH radical can travel only 2 cm in the plasma reactor itself before reacting with SiH_4 and has approximately five collisions within this distance.

Assuming that Θ_R has been thermalized to the gas temperature, the remaining issue is why Θ_T is significantly higher and has not, therefore, thermalized to the gas temperature. Although not fully understood, we can address some possibilities for this difference. First, there are no direct data available on the relaxation of the translational temperature of SiH created by electron-induced dissociation of SiH_4. A difference in relaxation rate for the rotational and translational temperature is therefore not excluded, suggesting it is possible that Θ_T has not yet completely equilibrated with Θ_R and the ambient gas temperature. Second, the measurements by Schmitt et al. were performed under conditions that are very different from ours and are also less appropriate for the commonly used rf capacitively or inductively coupled plasma reactors. The experiments by Schmitt et al. were performed in the postdischarge of a dc multipole reactor, with an average electron energy of 70 eV.[14] This might lead to differences in the measured relaxation rates and can also affect the rotational excitation of the reaction products of SiH_4.

A third possibility for the difference in temperatures is suggested by considering the gas-phase reactivity of SiH. As noted above, SiH radicals are very reactive with SiH_4, such that the SiH radicals probed in the molecular beam are produced relatively close to the extraction orifice. Radicals with higher translational temperatures will have fewer collisions than colder SiH; therefore, the SiH that survives and is extracted into the molecular beam could be relatively hot. These SiH radicals would also have less opportunity for full equilibration to Θ_R

and the gas temperature. To test this hypothesis, we are currently exploring the energetics of SiH radicals formed in mixed gas plasmas.[48] Finally, although it is uncommon for rotational and translational energies to be mismatched in molecular fragments of dissociation processes, it is not unprecedented. For example, photodissociation of CH_3I results in energy disposal predominately into translational motion of the methyl fragment (~90%), with very little placed in internal modes of the CH_3, primarily vibrational excitation in the methyl umbrella mode.[49] Hence, although not strictly parallel to our system, the difference in kinetic and rotational temperatures reported here could be entirely the result of the dynamical history of the dissociation processes for SiH_4 and Si_2H_6 in the plasma.

Returning to the issue of energy dissipation in SiH_4 and Si_2H_6 plasmas, note that the applied rf power can be used for fragmentation of the parent gas molecules and/or for translational, rotational, and vibrational heating of the plasma species. Assuming that Θ_R for SiH is equal to the average gas temperature in the plasma, it can be concluded that the increase in rf power does not lead to translational and rotational heating of the plasma species. Our LIF measurements indicate that at higher rf powers, more energy is used for the dissociation of SiH_4 and Si_2H_6. Furthermore, a considerable amount of the power can be dissipated by vibrational heating of the gas, whereas the transfer of vibrational energy to rotational or translational energy is small.[19,50] This type of energy dissipation cannot, however, be directly addressed with the present results.

Finally, we note that the energy partitioning found for the silylidyne radical is somewhat different from other species we have studied with IRIS. Specifically, measurements on NH_2 in NH_3 plasmas have shown a much lower kinetic translational temperature (~500 K) that increased considerably with power (~30% from 50 to 150 W), whereas the LIF intensity increased less than 15% over the same change in rf power.[15,17] The additional power must, therefore also be used for heating of the NH_2 in this system. Similarly, we observe an increase in Θ_T with rf power for OH in a $TEOS/O_2$ plasma.[16] Here, however, the change is not as pronounced (~15% from 85 to 115 W) and may be related to the mechanism for formation of OH in this system, namely H atom abstraction by oxygen atoms. Furthermore, Θ_R in this system is significantly lower than Θ_T, similar to the present work. Interestingly, Θ_R is nearly identical to Θ_T for OH radicals formed in a 100% H_2O plasma,[21,51] as expected for simple unimolecular bond rupture experiments where the potential energy barrier is small. Thus, the differences observed between Θ_R and Θ_T for SiH in both SiH_4 and Si_2H_6 plasmas are likely linked to the mechanism for formation as well as energy dissipation in the plasma.

IV. Conclusions

The surface reaction probability of SiH radicals produced in various silane- and disilane-based plasmas that are mixed with H_2, N_2, NH_3, or CH_4 has been measured by the IRIS method. A surface reaction probability of nearly unity, 0.96 ± 0.04, has been observed for SiH on the a-Si:H, μc-Si:H, a-SiN_x:H, and a-SiC_x:H film surfaces, independent of the gas mixture and plasma conditions applied. From this invariability and from a comparison to MD simulations of the surface interaction of SiH with a-Si:H, we conclude that sticking is likely the only surface reaction of SiH and that our measurements thus represent the SiH sticking probability of the materials studied. This very high sticking probability suggests that the silylidyne radical has a significant influence on the properties of the silicon-based films, even when the SiH density in the plasma is very low.

In addition, the SiH velocity in the molecular beam of the IRIS experiment was used to determine the kinetic translational temperature of SiH in the plasma, and the SiH rotational temperature was extracted from the measured rotational spectrum of SiH in the molecular beam. Both the Θ_T and Θ_R of SiH are essentially independent of applied rf plasma power (5−100 W) and are essentially equal in both SiH_4 and Si_2H_6 plasma systems. The measured translational temperature of ~1200 K is, however, considerably higher than the rotational temperature of ~600 K. This high kinetic translational temperature for SiH is likely caused by the excess energy released in the electron impact dissociation process of SiH_4 or Si_2H_6. Possible explanations for the lower rotational temperature have been addressed along with certain aspects of the power dissipation in the inductively coupled SiH_4 and Si_2H_6 plasmas.

Acknowledgment. Financial support for this research was provided by the Office of Naval Research (N00014-95-0644) and from the National Science Foundation (CHE-951157). W.K. gratefully acknowledges the financial support from the Eindhoven University of Technology in The Netherlands.

References and Notes

(1) Bruno, G.; Capezzuto, P.; Cicala, G. Chemistry of Amorphous Silicon Deposition Processes: Fundamental and Controversial Aspects. In *Plasma Deposition of Amorphous Silicon-Based Materials*; Bruno, G.; Capezzuto, P.; Madan, A., Eds.; Academic Press: San Diego, 1995; pp 1−62.

(2) Grill, A. *Cold Plasma in Materials Fabrication*; IEEE Press: Piscataway, NJ, 1994.

(3) Hamakawa, Y.; Ma, W.; Okamoto, H. Amorphous-Silicon-Based Devices. In *Plasma Deposition of Amorphous Silicon-Based Materials*; Bruno, G.; Capezzuto, P.; Madan, A., Eds.; Academic Press: San Diego, 1995; pp 283−314.

(4) Kakinuma, H.; Mohri, M.; Tsuruoka, T. *Jpn. J. Appl. Phys.* **1992**, *31*, L1392.

(5) Lee, K. R.; Sundaram, K. B.; Malocha, D. C. *J. Mater. Sci.* **1993**, *4*, 283.

(6) Meneve, J.; Dekempeneer, E.; Wegener, W.; Smeets, J. *Surf. Coat. Technol.* **1996**, *86*−*87*, 617.

(7) Hertl, M.; Jolly, J. *J. Phys. D*: *Appl. Phys.* **2000**, *33*, 381.

(8) Perrin, J.; Shiratani, M.; Kae-Nune, P.; Videlot, H.; Jolly, J.; Guillon, J. *J. Vac. Sci. Technol. A* **1998**, *16*, 278.

(9) Booth, J. P. *Plasma Sources Sci. Technol.* **2000**, *8*, 249.

(10) Shiratani, M.; Kawasaki, H.; Fukuzawa, T.; Watanabe, Y.; Yamamoto, Y.; Suganuma, S.; Hori, M.; Goto, T. *J. Phys. D* **1998**, *31*, 776 1998.

(11) Chantry, P. J. *J. Appl. Phys.* **1987**, *62*, 1141.

(12) Ho, P.; Breiland, W. G.; Buss, R. J. *J. Chem. Phys.* **1989**, *91*, 2627.

(13) McCurdy, P. R.; Bogart, K. H. A.; Dalleska, N. F.; Fisher, E. R. *Rev. Sci. Instrum.* **1997**, *68*, 1684.

(14) Schmitt, J. P. M.; Gressier, P.; Krishnan, M.; de Rosny, G.; Perrin, J. *Chem. Phys.* **1984**, *84*, 281.

(15) McCurdy, P. R.; Venturo, V. A.; Fisher, E. R. *Chem. Phys. Lett.* **1997**, *274*, 120.

(16) Bogart, K. H. A.; Cushing, J. P.; Fisher, E. R. *J. Phys. Chem. B* **1997**, *101*, 10016.

(17) McCurdy, P. R.; Butoi, C. I.; Williams, K. L.; Fisher, E. R. *J. Phys. Chem. B* **1999**, *103*, 6919.

(18) Perrin, J. *J. Phys. D*: *Appl. Phys.* **1993**, *26*, 1662.

(19) Perrin, J.; Leroy, O.; Bordage, M. C. *Contrib. Plasma Phys.* **1996**, *36*, 3.

(20) Scott, B. A.; Brodsky, M. H.; Green, D. C.; Kirby, P. B.; Plecenik, R. M.; Simonyl, E. E. *Appl. Phys. Lett.* **1980**, *37*, 725.

(21) Perrin, J.; Roca, P.; Cabarrocas, I.; Allain, B.; Friedt, J.-M. *Jpn. J. Appl. Phys.* **1988**, *27*, 2041.

(22) Patterson, G. N. *Introduction to the Kinetic Theory of Gas Flows;* University of Toronto Press: Toronto, 1971.

(23) Bauer, H.; Becker, K. H.; Duren, R.; Hubrich, C.; Meuser, R. *Chem. Phys. Lett.* **1984**, *108*, 560.

(24) This assumption has been verified on a number of occasions; see refs 16 and 17. The model also allows for an assumption of specular scattering.

(25) Pankov, A. Y.; Krylov, S. Y.; van Duijn, E. J.; Hermans, L. J. F. *J. Chem. Phys.* **2000**, *112*, 8680.

(26) Fisher, E. R.; Ho, P.; Breiland, W. G.; Buss, R. J. *J. Phys. Chem.* **1993**, *97*, 10287.

(27) Fisher, E. R.; Ho, P.; Breiland, W. G.; Buss, R. J. *J. Phys. Chem.* **1992**, *96*, 9855.

(28) Luque J.; Crosley, D. R. Lifbase: Database and Spectral Simulation Program (Version 1.5), SRI international report MP 99-099, 1999.

(29) Walkup, R.; Avouris, Ph.; Dreyfus, R. W.; Jasinski, J. M.; Selwyn, G. S. *Appl. Phys. Lett*. **1984**, *45*, 372.

(30) Huber, K. P.; Herzberg, G. *Constants of Diatomic Molecules*; Van Nostrand Reinhold: New York, 1979.

(31) An overview is given in Kessels, W. M. M.; Severens, R. J.; van de Sanden, M. C. M.; Schram, D. C. *J. Appl. Phys.* **2000**, *87*, 3313.

(32) Robertson R. M.; Rossi, M. J. *Appl. Phys. Lett*. **1989**, *54*, 185; *J. Chem. Phys.* **1989**, *91*, 5037.

(33) Ramalingam, S.; Maroudas, D.; Aydil, E. S. *Appl. Phys. Lett*. **1998**, *72*, 578.

(34) Ramalingam, S.; Maroudas, D.; Aydil, E. S. *J. Appl. Phys.* **1998**, *84*, 3895.

(35) Ramalingam, S.; Mahalingam, P.; Aydil, E. S.; Maroudas, D. *J. Appl. Phys*. **1999**, *86*, 5497.

(36) Ramalingam, S.; Maroudas, D.; Aydil, E. S. *J. Appl. Phys.* **1999**, *86*, 2872.

(37) Robertson, R.; Gallagher, A. *J. Appl. Phys.* **1986**, *59*, 3402.

(38) Matsuda, A. *J. Vac. Sci. Technol. A* **1998**, *16*, 365.

(39) Nomura, H.; Akimoto, K.; Kono, A.; Goto, T. *J. Phys. D* **1995**, *28*, 1977.

(40) Kae-Nune, P.; Perrin, J.; Guillon, J.; Jolly, J. *Plasma Sources Sci. Technol*. **1995**, *4*, 250.

(41) Hertl, M.; Dorval, N.; Leroy, O.; Jolly, J.; Péalat, M. *Plasma Sources Sci. Technol*. **1998**, *7*, 130.

(42) Tachibana, K.; Mukai, T.; Harima, H. *Jpn. J. Appl. Phys., Part 2* **1991**, *30*, L1208.

(43) Kessels, W. M. M.; Hoefnagels, J. P. M.; Boogaarts, M. G. H.; Schram, D. C.; van de Sanden, M. C. M. *J. Appl. Phys*. **2001**, *89*, 2065.

(44) Doughty, D. A.; Doyle, J. R.; Lin, G. H.; Gallagher, A. *J. Appl. Phys*. **1990**, *67*, 6220.

(45) Kessels, W. M. M.; Severens, R. J.; Smets, A. H. M.; Korevaar, B. A.; Adriaenssens, G. J.; Schram, D. C.; van de Sanden, M. C. M. *J. Appl. Phys*. **2001**, *89*, 2404.

(46) Matsumi, Y.; Hayashi, T.; Yoshikawa, H.; Komiya, S. *J. Vac. Sci. Technol. A* **1986**, *4*, 1786.

(47) Futako, W.; Takagi, T.; Nishimoto, T.; Kondo, M.; Shimizu, I.; Matsuda, A. *Jpn. J. Appl. Phys*. **1999**, *38*, 4535.

(48) Zhang, J.; Fisher, E. R., unpublished work.

(49) Hammerich, A. D.; Manthe, U.; Kosloff, R.; Meyer, H.-D.; Cederbaum, L. S. *J. Chem. Phys*. **1994**, *101*, 5623; Ogorzalek Loo, R.; Haerri, H.-P.; Hall, G. E.; Houston, P. L. *J. Chem. Phys*. **1989**, *90*, 4222, and references therein.

(50) Capitelli, M.; Gorse, C.; Winkler, R.; Wilhelm, J. *Plasma Chem. Plasma Process*. **1988**, *10*, 419.

(51) Buss, R. J.; Ho, P. *IEEE Trans. Plasma Sci*. **1996**, *24*, 79.